Collision frequency of electrons in laser excited small clusters

2009 J. Phys. A: Math. Theor. 42 214048

(http://iopscience.iop.org/1751-8121/42/21/214048)

J. Phys. A: Math. Theor. **42** (2009) 214048 (8pp) doi:10.1088/1751-8113/42/21/214048

Collision frequency of electrons in laser excited small clusters

Thomas Raitza[1], Heidi Reinholz[1,2], Gerd Röpke[1] and Igor Morozov[3]

[1] Institut für Physik, Universität Rostock, 18055 Rostock, Germany
[2] University of Western Australia, UWA, Perth, 6009 WA, Australia
[3] Joint Institute for High Temperatures of RAS, Izhorskaya, 13, Building 2, Moscow 125412, Russia

E-mail: thomas.raitza@uni-rostock.de

Received 23 October 2008, in final form 28 January 2009
Published 8 May 2009
Online at stacks.iop.org/JPhysA/42/214048

Abstract
Laser excited small metallic clusters are simulated using classical pseudo potential molecular dynamics simulations. Time-dependent distribution functions are obtained from the electron and ion trajectories in order to investigate plasma properties. The question of local thermodynamic equilibrium is addressed, and size effects are considered. Results for the electron distribution in phase space are given, which are interpreted within equilibrium statistical physics. Momentum autocorrelation functions were calculated for different cluster sizes and for different expansion states from the expanding system after the laser–cluster interaction. A resonance behaviour of the autocorrelation function in finite systems was observed. First, results concerning collision frequencies in small clusters are given.

PACS numbers: 31.15.Qg, 34.10.+x, 36.40.−c, 36.40.Gk, 36.40.Vz, 36.40.Wa, 52.20.Fs, 52.25.−b, 52.25.Fi, 52.25.Mq, 52.25.Os, 52.27.+j, 52.27.Gr, 52.27.Jt, 52.38.−r, 52.38.Dx, 52.50.Jm, 52.65.−y, 52.65.Yy, 72.15.Nj, 73.22.Lp, 78.67.−n

(Some figures in this article are in colour only in the electronic version)

1. MD simulation of laser excited clusters

Recently, experiments with laser excited small clusters [1] are in progress. Applying laser intensities of 10^{13}–10^{16} Wcm^{-2}, electrons become delocalized and ionization sets in. An electron cloud is bound to the ionic structure of the cluster, forming a nano plasma. Using pump–probe experiments [2], the dependence of enhanced absorption in nano plasmas on the time delay between pump and probe pulses was investigated. To understand the nano-plasma interactions, theoretical investigations of optical properties are of interest.

The dipole resonance behaviour of finite sodium systems in the ground state was considered, see [3]. Solving the Vlasov equation via PIC simulations [4] of pump–probe schemes, the resonant and non-resonant absorption of small sodium systems was calculated and the ionization dynamics was investigated. The ionization processes were modelled [5] for rare gas clusters of several thousand atoms via molecular dynamics (MD) simulations taking into account electron collisions. Collision absorption processes for very large systems were investigated [6] via hydrodynamical simulations.

For a bulk plasma, analytical calculations as well as MD simulations of autocorrelation functions have been done [7–9] to derive optical properties. Since these properties are sensitively dependent on the plasma temperature, density and ionization degree, their measurement can serve as a diagnostic tool.

Firstly, calculations of optical properties for finite systems were presented by Reinholz *et al* [10, 11]. Results for optical response taking MD calculations of laser excited sodium clusters of different sizes were compared with each other and with bulk systems. A main issue is to infer the properties of the finite plasma from measured spectra.

Finite systems are investigated, using MD simulations based on the method by Suraud [12] without periodic boundary conditions, in contrast to MD simulations of bulk systems. Sodium clusters of different sizes were treated, consisting of shells of icosahedrons. In the ground state, sodium atoms are represented via one electron on top of a singly charged ion. MD simulations were performed, using an error-function pseudo potential for the interaction between the particles (i, j denoting species electron and ion)

$$V_{\mathrm{erf}}(r_{ij}) = \frac{Z_i Z_j e^2}{4\pi\varepsilon_0 r_{ij}} \operatorname{erf}\left(\frac{r_{ij}}{\lambda}\right), \tag{1}$$

where Z_i is the charge of the ith particle. The electrons are charged negatively and the sodium ions are singly positively charged. The potential parameter $\lambda = 6.02 a_{\mathrm{B}}$ was chosen in order to reproduce the correct ionization energy $I_{\mathrm{P}} = V_{\mathrm{ei}}(r \to 0) = -5.1$ eV for sodium in the ground state when the electrons are situated on top of the ions.

2. Nano plasma properties of small clusters

Sodium clusters up to 309 atoms were investigated, irradiated with a $\cos^2$ laser pulse of 100 fs duration and maximum intensity of $I = 10^{12}$ Wcm^{-2}. In order to characterize the nano plasma after laser irradiation, single time properties like temperature and density will be derived from phase space coordinates which have been calculated within our MD simulations. To further analyse the nano plasma, we introduce the correlation parameter $\Gamma = e^2/(4\pi\varepsilon_0 d k_{\mathrm{B}} T_{\mathrm{e}})$, with the mean distance of the free electrons $d = (3/(4\pi n_{\mathrm{e}}))^{1/3}$. It relates the temperature to the interaction strength. The degeneracy parameter $\Theta = 2m_{\mathrm{e}} k_{\mathrm{B}} T_{\mathrm{e}}/(\hbar^2(3\pi n_{\mathrm{e}}))^{3/2}$ indicates the quantum properties of the respective ideal electron gas. Using MD simulation techniques, the results are valid only for plasmas, which are non-degenerate ($\Theta \gtrsim 1$) and almost ideal ($\Gamma \approx 1$). The Debye length $\lambda_{\mathrm{D}} = \sqrt{\varepsilon_0 k_{\mathrm{B}} T_{\mathrm{e}}/(e^2 n_{\mathrm{e}})}$ gives the screening length of the electron cloud.

2.1. Temperature of excited electrons

The momentum distribution of the electrons can be calculated at each time step of the expanding cluster system. As a result of 150 MD simulations for a Na_{309} cluster, figure 1 shows the average momentum distribution at different times after laser irradiation onset. A Boltzmann distribution is fitted to the simulations in each case. In this way, plasma temperatures can be

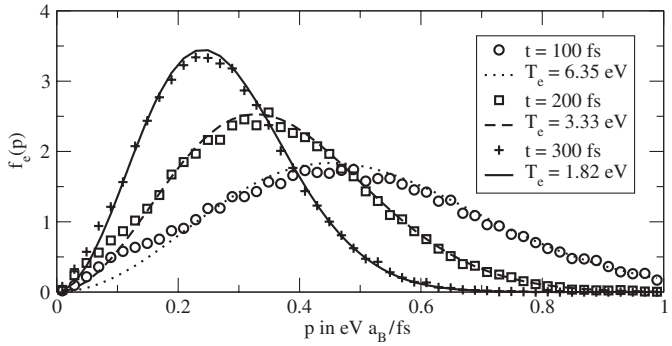

Figure 1. Particle ensemble averaged electron momentum distribution of the Na_{309} cluster at different times after onset of the 100 fs long $\cos^2$ laser pulse (symbols) and a Boltzmann fit (lines), respectively.

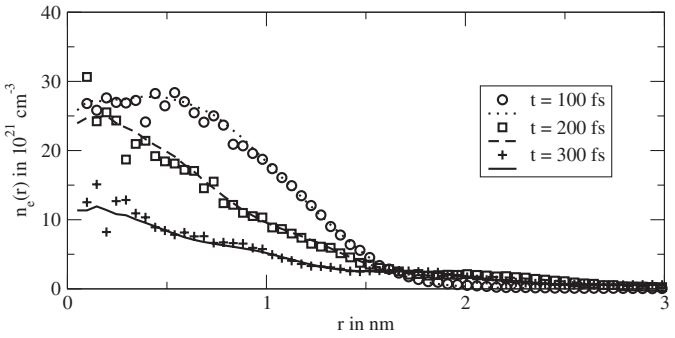

Figure 2. Electron density profile for the Na_{309} at different times after onset of the 100 fs long $\cos^2$ laser pulse. The electron gas is non-degenerate ($\Theta \gtrsim 1$) at all times.

well defined for all times from about 150 fs after laser onset. Before, there are significant deviations from the Boltzmann behaviour, in particular for small momenta. The concept of local thermal equilibrium might not be valid in this time range.

The electron temperature decreases due to cluster expansion. Looking for the distribution of each component of the momentum (p_x, p_y, p_z) separately, we found isotropy of the momentum distribution within an uncertainty of 10%.

2.2. Electron density profile inside the cluster

Now we investigate the electron density within the cluster. An ensemble of 150 MD simulation runs was taken here as well. The radial dependence of the electron density is shown in figure 2 for different times after the laser irradiation onset. In the outer region, the density decreases. With increasing expansion of the cluster, the plateau in the centre of the cluster vanishes and the electron gas becomes more dilute. The radial distribution strongly depends on the inhomogeneous expansion of the ionic shells.

We now want to consider a mean field potential $U(r)$ of the equilibrated electron system. It is determined from the forces

$$\vec{F}_j(\vec{r}_j) = \sum_{\substack{i=1,\\ i\neq j}}^{N_e} \vec{F}(|\vec{r}_i - \vec{r}_j|) + \sum_{i=1}^{N_i} \vec{F}(|\vec{r}_i - \vec{r}_j|). \tag{2}$$

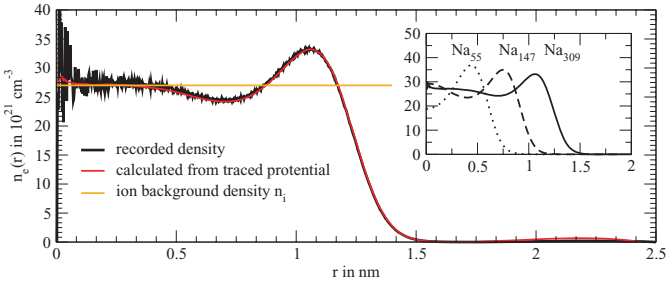

Figure 3. Electron density profiles of the Na_{309} at time instant $t_{freeze} = 100$ fs (black) as well as the calculated density from the traced effective potential (red). The inset shows the cluster size dependence of the density profile.

which are acting on a single electron j. Taking only the radial components $F_j(\vec{r}_j)$, and determining an averaged force $F(r) = \langle F_j(\vec{r}_j)\rangle$ from all electrons contained in a sphere of distance r from the centre, the mean field potential is calculated from

$$U(r) = \int_{\infty}^{r} \mathrm{d}r' F(r'). \tag{3}$$

The electron density follows from Boltzmann's law:

$$n_e(r) = n_0 \exp\left(\frac{U(r)}{k_B T_e}\right), \tag{4}$$

where $n_0 = N_e / \int_0^{\infty} \mathrm{d}r\, 4\pi r^2 \exp\left(U(r)/k_B T_e\right)$ is the normalization factor. The electron temperature T_e was taken from the momentum distribution, as discussed above. We obtain very good agreement with the direct analysis of the simulation data with respect to the central density as well as the surface profile, see figure 2. This fact strongly supports the assumption that local thermal equilibrium is well established for the nano plasma when looking at a time of 200 fs after laser irradiation onset.

For further understanding of this structure, we introduce a restricted MD simulation scheme. The ions are kept fixed at a certain time instant thus freezing particular thermodynamic properties. Assuming local thermal equilibrium of the electrons at all times, and due to the fixed ion geometry, one is able to replace the particle ensemble average by the time ensemble average of electrons using one single MD simulation run:

$$f_e(\vec{r}, \vec{p}) = \langle f_e(\vec{r}, \vec{p}, t)\rangle_t = \frac{1}{T}\int_0^T \mathrm{d}t f_e(\vec{r}, \vec{p}, t). \tag{5}$$

To characterize the plasma, it is important to know the central electron density, to be able to compare with bulk systems. To avoid inhomogeneities of the electron density in the centre, a new icosahedral ion geometry with average shell distance was taken, therefore guaranteeing the homogeneity of the ionic structure in the core region. The electrons were placed on top of the ions and a first kick pulse according to a kinetic energy of 1 eV was induced to every electron.

Results of calculations using the homogeneous ion structure via restricted MD simulation which corresponds to an ionic density of $n_i = 27 \times 10^{21}$ cm^{-3} and a temperature of $T_e = 1.2$ eV are shown in table 1.

The electron density profile n_e is shown in figure 3 compared with the calculation using an effective potential $U(r)$. An average over 10^6 time steps was taken. The effective

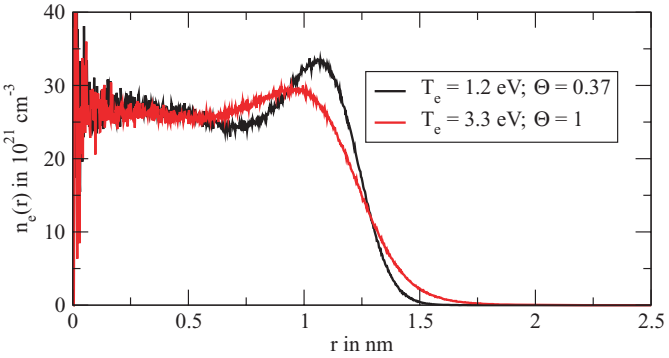

Figure 4. Electron density profiles of the Na_{309} at time $t_{freeze} = 100$ fs for two different temperatures.

Table 1. Results of restricted MD simulations with ion density $n_i = 27 \times 10^{21}$ cm^{-3} and electron temperature $T_e = 1.2$ eV: number of ions N_i; number of electrons N_e left inside the cluster; ionic cluster radius $r_c = \sqrt{5/3 \sum r_i^2}$; mean electron density $n_{e,mean}$ calculated from the number of electrons N_e and cluster radius r_c; central electron density $n_{e,centre}$; correlation parameter Γ; degeneracy parameter Θ; Debye length λ_D; degree of ionization α.

N_i	N_e	r_c (nm)	$n_{e,central}$ (10^{21} cm^{-3})	$n_{e,mean}$ (10^{21} cm^{-3})	Γ	Θ	λ_D (pm)	α
55	39	0.78	19	19.8	5.27	0.46	13.3	0.29
147	113	1.09	27	20.6	6.04	0.37	13.0	0.23
309	257	1.41	27	22.0	6.04	0.37	12.6	0.17

potential $U(r)$ was calculated in the same way as described for the expanding clusters. We obtain excellent agreement for the r_{309} cluster. The consistency of our calculations and the additional fact that the momentum distribution follows a Maxwell–Boltzmann distribution lead to the conclusion that the single time properties are given by equilibrium distributions when performing the restricted MD simulation. Similar results are obtained for full and restricted MD simulations at other parameters of the expanding clusters, so that local thermal equilibrium is established at 200 fs after the laser onset.

In contrast to the homogeneous positive background density, the electron density shows oscillations. Comparing different cluster sizes, see the inset of figure 3, these density oscillations are large near the surface. With increasing cluster size, a nearly constant electron density is established in the central region, which coincides with the ion density, so that we conclude that bulk properties are seen there.

To analyse the origin of the density oscillations at the surface, different temperatures were considered. Increasing the temperature of the Na_{309} to $T_e = 3.3$ eV ($\Theta = 1$), the density oscillation is reduced, see figure 4. Going towards lower temperatures, we have found that the oscillatory behaviour is more pronounced and a shell structure emerges which indicates the onset of a crystallization process in a strongly coupled Coulomb system (if treated classically). Investigating dusty plasmas with a jellium model for the ionic background potential and for $\Gamma > 80\,000$ [13], crystallization effects into shells were found at low temperatures.

Oscillatory electron density behaviour was also found for trapped quantum systems [14] as well as from quantum calculations of degenerate electron gases at surfaces [15]. In the

latter case, the wave number, which results from a modified Thomas–Fermi approximation, is dependent on temperature.

It was shown that a constant density plateau appears using a homogeneous ionic background density. The differences of the electron density profiles at certain time instants result from the expansion behaviour of the clusters depending on the cluster size. The surface profile results from the temperature-dependent crystallization of electrons. The density and the temperature were determined for every time instant. This allows us to characterize the nano plasma for 300 fs after laser interaction. For the smallest investigated Na_{55} cluster, no plateau is formed since the density profile is affected by the cluster surface.

3. Correlation function of excited electrons

We have shown that after laser–cluster interaction a nano plasma is performed in local thermal equilibrium. This is characterized by temperature $T_e(t)$ and density profile $n_e(r, t)$ which are obtained from single time distribution functions.

To calculate response properties, in particular optical absorption, two time correlation functions have to be considered. We investigate the momentum autocorrelation function (ACF) for a restricted MD simulation, taking the ions at fixed positions:

$$K(t) = \langle P_e(0), P_e(t)\rangle = \frac{1}{N_\tau}\sum_{i=1}^{N_\tau} P_e(i\tau)P_e(t+i\tau). \tag{6}$$

Here $P_e(t)$ is the total momentum of all electrons inside the cluster. The momentum ACF was calculated for a laser excited Na_{309} cluster after 100 fs, i.e. immediately after the irradiation with the $\cos^2$ laser profile. The Laplace transform of the momentum ACF

$$\tilde{K}(\omega) = \int_0^\infty \mathrm{d}t\, \mathrm{e}^{\mathrm{i}\omega t} K(t) \tag{7}$$

is a complex quantity. The real part is shown in figure 5 for parameter values, given in table 2.

From the fluctuation dissipation theorem [16], one can derive the following relation between current or momentum ACF and electrical conductivity:

$$\sigma(\omega) = \frac{1}{\Omega_0 k_B T_e}\langle J_{\mathrm{long}}, J_{\mathrm{long}}\rangle_\omega = \frac{n_e e^2}{m_e}\tilde{K}(\omega). \tag{8}$$

In bulk systems, $\tilde{K}(\omega)$ is peaked around the plasma frequency ${\omega_{\mathrm{pl}}}^2 = e^2 n_e/(m_e\varepsilon_0)$ and we can take collisions into account by generalized Drude formula

$$\sigma(\omega) = \frac{\epsilon_0\omega_{\mathrm{pl}}^2\omega}{-\mathrm{i}\left(\omega^2 - \omega_{\mathrm{pl}}^2\right) + \omega\nu_B(\omega)}, \tag{9}$$

where $\nu_B(\omega)$ is the bulk dynamical collision frequency. Using (7), the dynamical collision frequency can be calculated via momentum ACF:

$$\nu_B(\omega) = \frac{1}{\tilde{K}(\omega)} + \mathrm{i}\left(\omega - \frac{\omega_{\mathrm{pl}}^2}{\omega}\right). \tag{10}$$

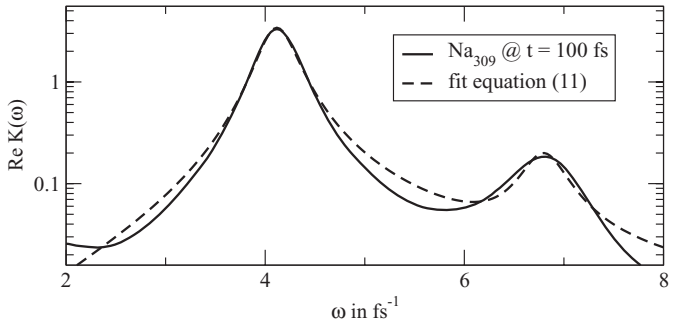

Figure 5. MD calculation of Laplace transformed momentum ACF of the Na_{309} cluster (solid line) with parameters given in the first line of table 2 and two Lorentzian fits (dotted line) using 11.

Table 2. Resonance and collision frequencies for the Na_{55} cluster in comparison to the Na_{309} cluster at different times (100 fs, 150 fs and 200 fs).

$n_e\,10^{21}$ (cm^{-3})	T_e (eV)	ω_1 (fs^{-1})	ν_1 (fs^{-1})	ω_2 (fs^{-1})	ν_2 (fs^{-1})
		Na_{55}^{11+} cluster			
17.2	1.2	3.8	0.26	6.2	0.52
11.2	0.9	3.1	0.22	5.3	0.62
6.7	0.7	2.4	0.26	4.4	1.04
		Na_{309}^{46+} cluster			
18.5	3.0	4.1	0.39	6.8	0.63
12.4	2.4	3.1	0.34	5.4	0.91
7.5	1.9	2.3	0.31	4.1	1.27

For a Na_{309} cluster with frozen ions at $t_{\text{freeze}} = 100$ fs, two broadened resonance structures are visible in $\tilde{K}(\omega)$, as shown in figure 5. A fit (dashed line) of the simulated momentum ACF (solid line) Re $\tilde{K}(\omega)$ is also shown using a linear combination of two Lorentzians

$$\tilde{K}(\omega) = \frac{K_1\omega}{\nu_1\omega - \mathrm{i}\left(\omega^2 - \omega_1^2\right)} + \frac{K_2\omega}{\nu_2\omega - \mathrm{i}\left(\omega^2 - \omega_2^2\right)}, \tag{11}$$

where ν_1 and ν_2 as well as ω_1 and ω_2 are used to fit the position and the width of the resonance peaks. The parameters K_1 and K_2 determine the strength of the resonances. In table 2, results are compared for the Na_{55} and Na_{309} clusters for different times after laser irradiation. The temperature decreases with time and the system becomes more dilute, which results in smaller resonance frequencies for both cluster sizes. However, the collision frequency is increasing for the second resonance. Comparing the collision frequency of both cluster sizes, an increase with bigger cluster size is observed.

4. Conclusion and outlook

The methods developed to investigate homogenous non-ideal plasmas have been applied to finite nano plasmas, produced by laser irradiation of clusters. It has been shown that local thermal equilibrium is established shortly after the laser irradiation has been switched

off. Using restricted MD simulations, we determined single time properties (density and momentum distribution) as well as two time properties, in particular the momentum ACF spectrum. The single time properties are well reproduced from equilibrium statistics. The momentum ACF shows a peak structure. Further investigations are needed to explain the position of the peaks that indicate the frequencies of excitation modes of the cluster.

We determined frequency-dependent damping rates by Lorentzian fits to the excitation spectrum. First results of size-dependent collision frequencies were presented. More systematic investigations are needed to analyse the size effects in the collision frequency, what will be the subject of future work.

Acknowledgments

The authors gratefully acknowledge financial support by the Deutsche Forschungsgemeinschaft within the Sonderforschungsbereich SFB 652. IM acknowledges the 'Dynasty' Foundation.

References

[1] Döppner T, Diederich T, Przystawik A, Truong N X, Fennel T, Tiggesbäumker J and Meiwes-Broer K-H 2007 *Phys. Chem.* **9** 4639
[2] Fennel T, Döppner T, Passig J, Schaal C, Tiggesbäumker J and Meiwes-Broer K-H 2007 *Phys. Rev. Lett.* **98**
[3] Kümmel S, Brack M and Reinhard P-G 2000 *Phys. Rev.* B **62**
[4] Köhn J, Redmer R, Meiwes-Broer K-H and Fennel T 2008 *Phys. Rev.* A **77**
[5] Fennel T, Ramunno L and Brabec T 2007 *Phys. Rev. Lett.* **99**
[6] Hilse P, Schlanges M, Bornath T and Kremp D 2005 *Phys. Rev.* E **71**
[7] Reinholz H, Redmer R, Röpke G and Wierling A 2000 *Phys. Rev.* E **62** 5648
[8] Morozov I, Reinholz H, Röpke G, Wierling A and Zwicknagel G 2005 *Phys. Rev.* E **71** 066408
[9] Reinholz H, Morozov I, Röpke G and Millat T 2004 *Phys. Rev.* E **69** 066412
[10] Reinholz H, Raitza T and Röpke G 2007 *Int. J. Mod. Phys.* B **21** 2460
[11] Reinholz H, Raitza T and Röpke G *Int. J. Mod. Phys.* B at press
[12] Belkacem M, Megi F, Reinhard P-G, Suraud E and Zwicknagel G 2006 *Eur. Phys. J.* D **40** 247
[13] Totsuji H, Ogawa T, Totsuji C and Tsuruta K 2005 *Phys. Rev.* E **72** 036406
[14] Bonitz M *et al* 2008 *Phys. Plasmas* **15** 055704
[15] Bartos I, Kolar M and Paasch G 1983 *Phys. Status Solidi* B **115** 437
[16] Reinholz H 2006 *Ann. Phys. (Fr)* **30** 4–5
[17] Ramunno L, Jungreuthmayer C, Reinholz H and Brabec T 2006 *J. Phys. B: At. Mol. Opt. Phys.* **39** 4923